Oil & Gas Science and Technology – Rev. IFP, Vol. 65 (2010), No. 4, pp. 597-614

DOI: 10.2516/ogst/2009076

Dossier

CO_2 Storage in the Struggle against Climate Change
Le stockage du CO_2 au service de la lutte contre le changement climatique

First Modelling Results of the EM Response of a CO_2 Storage in the Paris Basin

B. Bourgeois and J.F. Girard

BRGM, Service Aménagement et Risques Naturels, BP 36009, 45060 Orléans Cedex 2 - France
e-mail: b.bourgeois@brgm.fr - jf.girard@brgm.fr

Résumé — Premières modélisations de la réponse EM d'un stockage de CO_2 dans le bassin Parisien — Nous étudions la possibilité d'utiliser les méthodes électriques/EM pour surveiller l'injection de CO_2 supercritique à 1700 m de profondeur dans un aquifère salin du Bassin Parisien (Carbonates du Dogger). Nous démontrons d'abord l'intérêt théorique des méthodes de résistivité pour une telle surveillance à l'aide des lois fondamentales de la pétrophysique dans les roches sédimentaires poreuses, en supposant que le CO_2 supercritique est un isolant parfait. Diverses combinaisons de sources et de capteurs sont discutées et il est conclu que le dispositif le plus performant consiste en une source de type galvanique (injection de courant dans le sol à l'aide d'une paire d'électrodes A et B) et d'une grille de capteurs électriques (et peut-être magnétiques) à la surface du sol.

Compte tenu de la profondeur et de la finesse des couches réservoir, l'injection du courant en profondeur est envisagée dans le but d'augmenter la densité de courant circulant dans la couche réservoir. L'injection ponctuelle à la profondeur du réservoir, dans une configuration de type « Mise À la Masse » (MAM), étant généralement impossible à cause de la présence de tubages métalliques dans les forages, nous avons étudié la possibilité d'utiliser ces mêmes tubages comme des longues électrodes distribuant le courant tout le long du forage. Ce type de source est dénommé « LEMAM » (Long Electrode Mise À la Masse), pour le distinguer du MAM conventionnel.

Des simulations numériques sont présentées à la fois pour le dispositif LEMAM et pour le dispositif « rectangle » (RECT), lequel emploie une injection de courant ponctuelle à la surface du sol. Le modèle géoélectrique utilisé est basé sur une zone proche du champ pétrolier de Saint-Martin-de-Bossenay (SMB), au sud-est du Bassin Parisien. La couche réservoir considérée dans cette étude est la formation de l'« Oolithe Blanche » (Dogger) qui a une épaisseur de 75 m et se situe à une profondeur de 1700 m sous la surface du sol. Dans les modèles présentés, le panache de CO_2 est simplifié en une plaque horizontale carrée de 2 km de côté et de 70 m d'épaisseur flottant au toit de l'aquifère réservoir. Une saturation uniforme en CO_2 égale à 80 % a été adoptée dans la plaque, ce qui représente un contraste de résistivité de 25 par rapport à l'aquifère initial.

Deux variantes du modèle avec des résistivités différentes pour l'aquifère sont comparées. Le cas d'une résistivité réaliste de 20 ohm.m donne une réponse électrique time-lapse inférieure au bruit de répétition estimé. Ce résultat décevant s'explique par le fait que la couche réservoir dans ce cas est loin d'être la plus conductrice du modèle ; par conséquent, elle est traversée seulement par une petite partie du courant injecté, d'où la faible réponse du CO_2. Une deuxième variante avec une résistivité plus favorable que la réalité, mais parfaitement réaliste pour un aquifère salin (1 ohm.m), donne une réponse électrique time-lapse de l'ordre de 6 % du champ initial, ce qui est bien supérieur au bruit de répétition estimé. Nous concluons donc que la méthode LEMAM est prometteuse pour surveiller un stockage de CO_2, à condition que l'aquifère réservoir soit suffisamment conducteur par rapport au reste de la série recoupée par les longues électrodes.

Abstract — First Modelling Results of the EM Response of a CO_2 Storage in the Paris Basin — *We study the feasibility of using electrical/EM methods for monitoring the injection of supercritical CO_2 at a depth of 1700 m in a saline aquifer of the Paris Basin (Dogger carbonates). We first establish the theoretical interest of resistivity methods for CO_2 monitoring through the basic laws of electrical physics in porous sedimentary rocks, assuming that supercritical CO_2 is a perfect insulator. Various combinations of EM sources and sensors are discussed and it is shown that the best type of array consists of a galvanic source (i.e. injection of current via a pair of electrodes A and B) and of a grid of electric (and possibly magnetic) sensors at the ground surface.*

Given the usual depth and thinness of CO_2 storage layers, current injection at depth was investigated in order to increase the current density in the reservoir and thus enhance the CO_2 response. Point injection at the reservoir depth in the so-called "Mise À la Masse" (MAM) configuration is generally impossible in deep wells due to the presence of metallic casings. Therefore, the possibility of using a deep metallic casing as a long electrode distributing the current all along a borehole is studied. This kind of source is named "LEMAM" (Long Electrode Mise À la Masse) in order to differentiate it from the conventional MAM.

Numerical simulations are presented for the LEMAM array and for the gradient or rectangle array (RECT), for which the current is injected by a pair of point electrodes at the ground surface. The geoelectric model used is based on an area close to the Saint-Martin-de-Bossenay (SMB) oilfield, in the south-east of the Paris Basin. The storage reservoir considered in this study is the 75-m-thick "Oolithe Blanche" formation (Mid Jurassic or Dogger, Bathonian age), located at a depth of about 1700 m below ground surface. In the models presented, the CO_2 plume is simplified to a square horizontal slab of 2 km side, 70 m thick, floating at the top of the oolite aquifer. A uniform CO_2 saturation of 80% is assumed, yielding a resistivity contrast of 25 with the initial reservoir.

Two variants of the model with different reservoir resistivities are compared. The first model is calculated with a realistic reservoir resistivity of 20 ohm.m, reflecting the low salinity of the aquifer in this part of the Basin (≈ 5 g/L of NaCl). With this model, the time-lapse electric response of the CO_2 plume is less than 0.5% of the initial electric field, which is below the estimated "repetition noise". This poor result can be explained by the fact that the reservoir, in this case, is far from being the most conductive layer of the model. As a consequence, only a minor part of the injected current is used for energizing the CO_2 plume: a rough calculation shows that only about 2% of the injected current crosses the reservoir, hence the poor response of the plume.

A second model is calculated with an idealistic reservoir resistivity of 1 ohm.m, corresponding to about 50-70 g/L of NaCl in the aquifer (though such salinity is not observed anywhere in the Dogger aquifer of the Paris Basin, it is common in many storage aquifers). With this favourable model, it is estimated that about 30% of the injected current crosses the reservoir and energizes the plume, resulting in a time-lapse electric response as high as 6% of the initial field, which is quite measurable. For comparison, the time-lapse electric response obtained with the same model for a surface current injection (RECT array) is only 2% of the initial field. With this same model, the time-lapse magnetic response obtained for the LEMAM injection is about 3% of the initial magnetic field.

We conclude that the LEMAM array is very promising for the resistivity monitoring of a CO_2 injection in a deep aquifer, provided that the water salinity is high enough for the reservoir to channel a significant fraction of the injected current (say >10%).

SYMBOLS, UNITS AND ABBREVIATIONS

$\boldsymbol{E}$	Electric field (V/m)
$\boldsymbol{H}$	Magnetic field (A/m)
ρ	Electrical resistivity (ohm.m)
σ	Electrical conductivity (S/m)
C	Longitudinal conductance, *i.e.* conductivity × thickness (S) for a 1D layer, conductivity × section (S.m) for a 2D cylinder
Φ	Porosity (m^3/m^3)
K	Hydraulic permeability (mD)
S_w	Water saturation (m^3/m^3)
V	Volume (m^3)
I	Current intensity (A)
EM	Electromagnetism
RECT	"Rectangle" array (also known as "gradient" array) consisting of two injection electrodes A and B nailed at the ground surface
MAM	"Mise À la Masse" array
LEMAM	"Long Électrode Mise À la Masse" array
SMB	Saint-Martin-de-Bossenay
FDB	Fontenay-de-Bossery

INTRODUCTION

Geological storage of CO_2 is presently considered as a viable means of reducing the amount of CO_2 released to the atmosphere. However, the public acceptance of this new concept is conditioned to the advent of reliable monitoring techniques capable to follow the progression of the CO_2 plume inside the reservoir and/or to early warn of possible escapes in the overburden. In particular, monitoring the extension of the CO_2 bubble during the injection is crucial for reservoir engineering since it allows validation of the predictive flow/transport models and readjustment of their parameters to agree with the observations.

In geophysics, 4D seismics has proven its great sensitivity and resolution on the Sleipner site, but it is admitted that the method is expensive and that it may not be applicable to all the reservoirs. Other cheaper method should thus be developed to allow a more frequent control of the injection. The resistivity of a porous rock being very sensitive to the pore fluid content, several teams have proposed to follow the variation of the electrical resistivity in order to monitor the CO_2 injection. This approach seems especially relevant in the case of a saline aquifer, where the introduction of CO_2 generates a strong increase of the resistivity.

DC electrical methods and low-frequency (diffusive) EM methods can thus be envisaged for monitoring the CO_2 injection, in complement to 4D seismic methods. The value of coupling resistivity methods with seismics is already widely recognized in hydrocarbon exploration, where marine CSEM and land TEM have experienced a very rapid growth since 2002. Moreover, the repeated, time-lapse implementation used in monitoring should provide much greater sensitivity and resolution than the single-time implementation used in exploration.

However, for storage efficiency and safety purposes, it is agreed that the reservoir should be deep enough for the CO_2 to be in a supercritical state: due to its relatively high density ($> 500\ kg/m^3$), supercritical CO_2 provides a better efficiency (smaller storage volume) and a better immunity against leakage through the caprock (due to reduced buoyancy) than gaseous CO_2. Assuming a geothermal gradient of 30°C/km, a surface temperature of 10°C and a standard hydrostatic pressure, CO_2 becomes supercritical at a depth of 700 m, but most envisaged reservoirs are much deeper (> 1500 m in the Paris Basin).

This situation makes it difficult to detect and monitor resistivity changes in the reservoir using standard electrical/EM methods operated from the surface. Logging and cross-well electrical/EM methods overcome this limitation, but they need wells reaching or exceeding the reservoir depth and compatible for such measurements in terms of completion, inter-well distance, etc.

In order to increase the efficiency of electrical/EM methods, we propose to bring the source closer to the CO_2 plume by using a pair of metal-cased boreholes, acting as long electrodes, to inject the electrical current at depth, and to measure the resulting EM field at the surface. We designate this array as LEMAM (for Long Electrode Mise À la Masse). The casings used for injection must reach the reservoir, but there is no other requirement on the well completions. The boreholes can be pre-existing in the case of a depleted hydrocarbon reservoir or drilled specially for monitoring purposes in the case of a saline aquifer. Though such array looks like DC, the EM designation is more appropriate since the inductive effects cannot be neglected at such large geometric scales, even at low frequency of the injected current (square waveform).

In the framework of the "Géocarbone-Monitoring" project (2006-2008) supported by the French Research Agency (ANR), one objective of BRGM was precisely to study the feasibility of electrical/EM methods for monitoring a deep CO_2 injection in the Paris Basin. Two aquifers were the possible targets of the study: the carbonate aquifer of the Dogger (oolitic limestone of Bathonian age), and the sandstone aquifer of the Keuper (Rhaetian age) several hundred meters below.

A favourable "sector" for CO_2 storage had previously been selected in the south-east of the Paris Basin *(Fig. 1)* within the "PICOREF" project(1) (2005-2006). Inside this sector, the area around Saint-Martin-de-Bossenay (SMB), is well documented until the Dogger series thanks to the vicinity of the SMB producing field, which extracts oil from upper Dogger carbonates (Dalle Nacrée and Comblanchien formations). These series are also well known due to the widespread geothermal exploitation of the Dogger aquifer in the surroundings of Paris.

For these reasons, we have focused our work on the Dogger formation and abandoned the deeper Triassic series for further projects. The selected study area is about 10 km west of the SMB oilfield *(Fig. 1)*, outside the oil-bearing structure, at a place where the porous carbonates are filled with brackish water. For convenience, we will also use the SMB acronym to designate this area and the associated model, but it must not be conjectured that we are studying a CO_2 injection in a depleted hydrocarbon reservoir: our study addresses the case of a saline aquifer.

1 ROCK PHYSICS

In a porous sedimentary formation with low clay content (condition likely to be true in most adequate storage formations), the electrical conduction is dominated by ionic migration within the interconnected pore channels (*i.e.* electrolytic conduction). The bulk conductivity of the rock is thus very sensitive to any insulating fluid phase existing within the pores (such as oil, gas or supercritical CO_2), because such a phase reduces the effective volume of water available for

(1) Supported by the French Ministry of Industry under RTPG network for Petroleum and Gas industry.

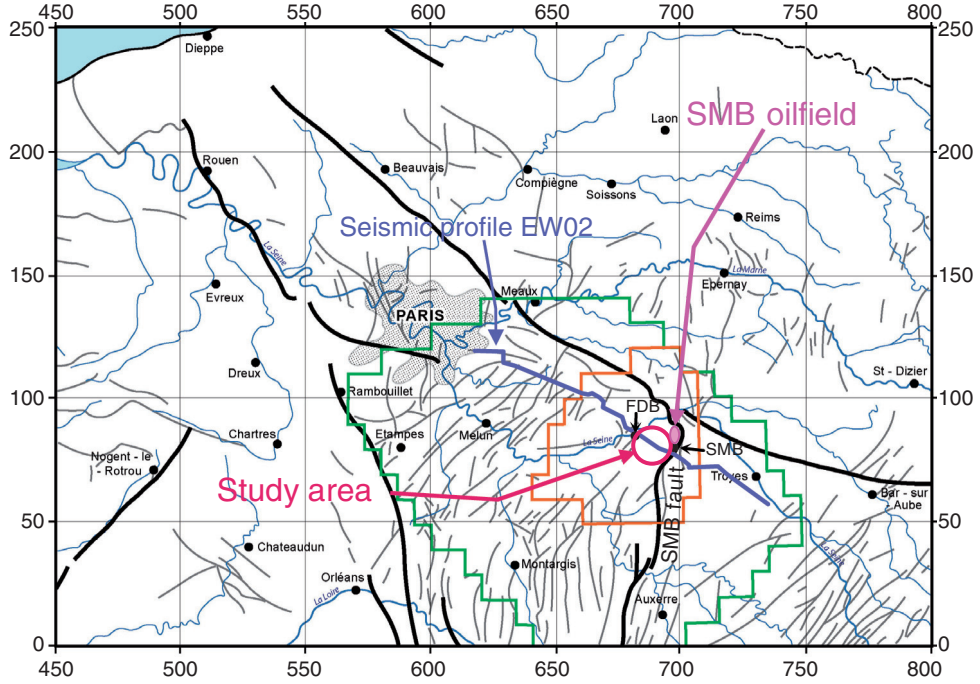

Figure 1
Map of the Paris Basin, showing the PICOREF region (in green), the PICOREF sector (in orange), the SMB oilfield and the selected study area (adapted from a figure by E. Brosse, IFP).

ionic transport, and thus radically decreases the rock conductivity. As a consequence, the replacement (even partial) of a conductive brine by CO_2 will significantly increase the bulk resistivity of the rock.

When the electrolytic conduction dominates, *e.g.* in a sandy formation with low clay content (or whatever the rock matrix if the interstitial brine is "sufficiently" conductive), the bulk conductivity of the rock is reasonably well described by the empirical Archie law (1942). The generalized form of this law, which is valid even when the sediment is not water-saturated (*i.e.* when insulating fluids coexist with the formation water within the pores), relates the conductivity σ of the rock to its porosity Φ, to the conductivity σ_w of the interstitial water, and to the water saturation S_w:

$$\sigma \approx \sigma_w \, \Phi^m \, S_w^n \quad (m \in [1.3, 3] \text{ and } n \in [1.7, 2.2]) \qquad (1)$$

where m and n are the cementation and saturation exponents (often close to 2), and where the water saturation S_w is defined as the volume fraction of electrolyte in the pore space:

$$S_w = V_{water}/V_{pores}$$

The rest of the porosity is supposed to be filled with insulating fluids: indeed one basic assumption underlying the Archie law is that liquid water (more or less saline and possibly mixed with other polar solvents) is the unique conductive solution in the pore space. As a matter of fact, no other conductive solution can be found outside the aqueous phase in a sedimentary rock. Supercritical CO_2, despite its powerful solvent properties, can be considered as an insulator like a gas (air, methane, etc.) or oil: though the literature is very scarce on this question, it can be conjectured that this property probably originates from the fact that CO_2 is a non-polar solvent.

The sum of the different fluid fractions being equal to one, in the most general case, S_w can be written as:

$$S_w = 1 - (S_{gas} + S_{oil} + S_{CO_2}) \qquad (2)$$

where S_{gas}, S_{oil} and S_{CO_2} represent respectively the volume fractions of gas (air, methane, etc), oil and supercritical CO_2 contained in the pore space. In the case of a CO_2 injection in a saline aquifer, S_{gas} and S_{oil} should normally be very small, so we can write:

$$S_w = 1 - S_{CO_2} \qquad (3)$$

From Equations (1) and (3), the bulk resistivity of the rock flooded with CO_2 can finally be expressed as:

$$\rho \approx \rho_w \, \Phi^{-m} \, (1 - S_{CO_2})^{-n} \qquad (4)$$

(where ρ and ρ_w are the inverses of σ and σ_w).

By setting the CO_2 saturation to zero, we derive the resistivity ρ_0 of the reservoir before CO_2 injection, *i.e.* at full water saturation:

$$\rho_0 \approx \rho_w \, \Phi^{-m}. \quad (5)$$

If we assume that the CO_2 injection modifies neither the resistivity ρ_w of the pore water nor the pore structure of the rock (reflected by the porosity Φ and by the cementation exponent m), the ratio of formulas (4) and (5) directly gives a very simple expression of the resistivity variation due to the CO_2 flood (fluid substitution) at a given point of the reservoir:

$$\rho/\rho_0 \approx (1 - S_{CO_2})^{-n}. \quad (6)$$

It should be noted that the previous assumption supposes a relatively short time interval (possibly less than a decade) after the start of CO_2 injection. In the long term, *i.e.* after several decades, this simplistic assumption may no longer be valid due to the chemical interactions between the CO_2 and the host formation (acidification of interstitial water, modification of the pore structure), interactions that can modify the water resistivity ρ_w, the porosity Φ and the cementation exponent m in Equation (4). For the moment, we have ignored these phenomena, firstly because they are negligible in the short term, and secondly because they are still badly known.

If the reservoir layer is sufficiently uniform, the ratio given by Equation (6) also represents the resistivity contrast between the CO_2 plume and the rest of the reservoir (CO_2-free area).

Equation (6) indicates that the bulk resistivity of the flooded rock regularly increases with the volume fraction of CO_2 injected in the pore space, as illustrated in Figure 2. It is worth noting that the relative increase (resistivity ratio) is independent of the rock porosity and of the water salinity (at least in the Archie model).

For our simulations, we have assumed a uniform CO_2 saturation of 80% within the plume (see later), which results in a multiplication of the initial aquifer resistivity by 25 (for $n = 2, S_{CO_2} = 0.8 \Rightarrow S_w = 0.2 \Rightarrow \rho/\rho_0 = 25$).

NB: In the presence of clay minerals, the Archie law is no longer rigorous and a more complex model has to be used (*e.g.* Waxman and Smits, 1968). For the moment, we consider that the Archie model is sufficiently accurate for the purpose of CO_2 monitoring in saline aquifers, since the high conductivity of the brine masks the effect of the clay particles and enables the Archie law to be verified at higher clay concentrations.

2 THE LEMAM ARRAY COMPARED WITH STANDARD DC ARRAYS

We have seen that the CO_2 bubble will show up as a resistive body in a conductive background (at least in the short term). According to Bourgeois *et al.* (2000), closed eddy currents cannot take place in such a target, since the "vortex mode" of EM induction can only appear in a conductive target. Therefore the EM response of a CO_2 plume can only be of galvanic type (*i.e.* current diversion around the plume), for which the best stimulation is supplied by the electric field *E*.

We thus conclude that the EM source for CO_2 monitoring should definitely be galvanic, consisting of a current injection into the ground *via* two electrodes A and B ("electric bipole"), since this kind of source mainly produces electric field – as opposed to a closed loop of current, which mainly produces magnetic field. In order to support our demonstration, it can be remarked that marine CSEM or land TEM methods, that were developed for hydrocarbon exploration, *i.e.* for detecting a resistive target in a conductive environment, effectively use galvanic sources.

Standard galvanic sources use point electrodes nailed at the ground surface to inject the current into the ground, like in the "rectangle" (or gradient) array depicted in Figure 3a. Given the usual depth and thinness of the reservoir layers, it was anticipated that the fraction of current flowing in the reservoir with this array would be very small.

The ideal array would be to inject the current directly at the reservoir depth, in a "Mise À la Masse" (MAM) configuration *(Fig. 3b)*, but this would need specific well completions with electrodes A and B buried behind the casings, and with these being non-conductive on a sufficient section above and below the electrodes: to our knowledge, such completions are only available at Ketzin, and their development will probably be curbed by cost considerations.

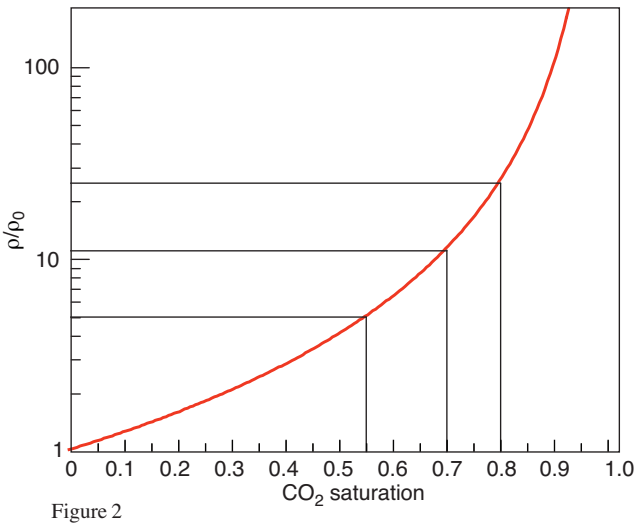

Figure 2

Resistivity contrast between a rock flooded with CO_2 and the same rock saturated with water (*i.e.* no gas or oil fraction before CO_2 injection) as a function of the CO_2 saturation, for exponent $n = 2$ in Equation (6) (clean sand). Three particular cases of fluid substitution have been highlighted: S_{CO_2} = 55%, 70% and 80%, for which the resistivity contrasts are respectively 5, 11 and 25.

We have thus investigated the possibility of using a pair of deep metallic casings to serve as long electrodes distributing the current continuously from the surface to the reservoir depth *(Fig. 3c)*. This injection array is possibly less effective than a true MAM, but is much more effective than a simple injection at the surface. If the saline reservoir aquifer is significantly more conductive than the other formations, it will channel most of the electric current at the reservoir depth, and thus the long-electrode injection will be equivalent to the MAM injection. In contrast, if other very conductive layers are intersected by the borehole, a significant part of the injected current will escape in these layers and the reservoir will be poorly energized. We have designated this distributed current injection as "LEMAM" (for Long Electrode Mise À la Masse).

For the purpose of CO_2 monitoring, we propose to combine the LEMAM injection of a square-wave alternating current with standard electric/magnetic field measurements at the ground surface (*i.e.* borehole-to-surface configuration). Following common practice, the electric field will be measured by the potential difference between two point electrodes at the surface (MN dipole), the *E* field in the MN direction being given by: $E_{//MN} \approx (V_M - V_N)/MN$. The electric field at the surface being horizontal (due to the infinite resistivity contrast at the air-earth interface), the electric vector will be measured by two perpendicular voltage dipoles (M*x*, N*x*) and (M*y*, N*y*). Three orthogonal magnetic sensors will be used to measure the magnetic vector.

This configuration differs from the Long Electrode Resistivity Tomography (LERT), advocated by Newmark *et al.* (2001) and Daily *et al.* (2004), which uses metal casings both for the current injection and for the voltage measurements. As the authors recognize, such an array gives an uncontrollable (generally poor) horizontal resolution, function of the density of available wells (externally imposed), and absolutely no vertical resolution – there is no way to determine the depth of a conductivity anomaly since the casing is nearly an equipotential line. In contrast, the use of point electrodes at the surface for the *E* measurement preserves a high horizontal resolution (controlled by the density of measuring stations) and a normal vertical resolution.

Since inductive effects may be significant at the great geometric scales involved in CO_2 monitoring, we will need to measure complex components (*i.e.* module and phase) of the electric/magnetic field vectors, which implies an adequate synchronization between the transmitter (Tx) and the receiver (Rx).

The surveys will be repeated at regular intervals, in a time-lapse approach. For each repetition, the time-lapse CO_2 response will be calculated as the electric (and possibly magnetic) field difference between the current iteration and the initial "baseline" measured before CO_2 injection.

To conclude this discussion, it may be useful to summarize in Table 1 the essential characteristics of the LEMAM array compared to the other possible arrays.

TABLE 1

Characteristics of four electric arrays that can be envisaged for CO_2 monitoring

Array	Current injection	*E*-field (voltage) measurement
RECT	Point electrodes at the surface	Point electrodes at the surface
MAM	Point electrodes at depth	Point electrodes at the surface
LEMAM	Long electrodes	Point electrodes at the surface
LERT	Long electrodes	Long electrodes

The use of long electrodes for current injection was already reported in the geophysical literature, mainly for exploration (very little for monitoring). In geothermal exploration, several teams used a single-well LEMAM injection in conjunction with measurements of the scalar electric potential (Kauahikaua *et al.*, 1980; Hatanaka *et al.*, 2005; Supriyanto *et al.*, 2005) or alternatively with measurements of the electric-field vector (Bourgeois *et al.*, 1983).

Again in geothermal exploration, Sill and Ward (1978) used a double-well LEMAM injection in conjunction with electric-field measurements. In every respect, their approach was very close to what we propose now for CO_2 monitoring, be it for the transmitter/receiver configuration, survey scale, frequency range, parameters retrieved, etc. The only difference with our proposal is that these authors were working in a single-time implementation instead of the repeated implementation that we intend to use in monitoring.

In hydrocarbon exploration, Rocroi and Koulikov (1985) introduced the TUBEL method (registered trade mark of CGG) which consisted of a double-well LEMAM injection and of dipole measurements of only the main electric component Ex (*i.e.* that component oriented in the AB direction).

Though giving interesting results, all these experiments underlined the same difficulty: in order to enhance the weak response of the deep 3D targets, it is necessary to reduce the observed field by an approximate response of the background (either calculated or measured with a different array). It is worth noting that this difficulty will automatically disappear when using the LEMAM array in a time-lapse implementation, since the reduction in this case will be done by a previous dataset obtained with the same Tx/Rx array (and not by a calculated model). This will mechanically eliminate the background regional field as well as most of the shallow responses. In fact, all the geoelectric features that did not vary between the two iterations will be eliminated in the differencing process. Only the volumes of varying resistivity should appear on the reduced data, in particular the areas were the CO_2 has (partly) replaced the initial brine, producing a sharp increase in the rock resistivity.

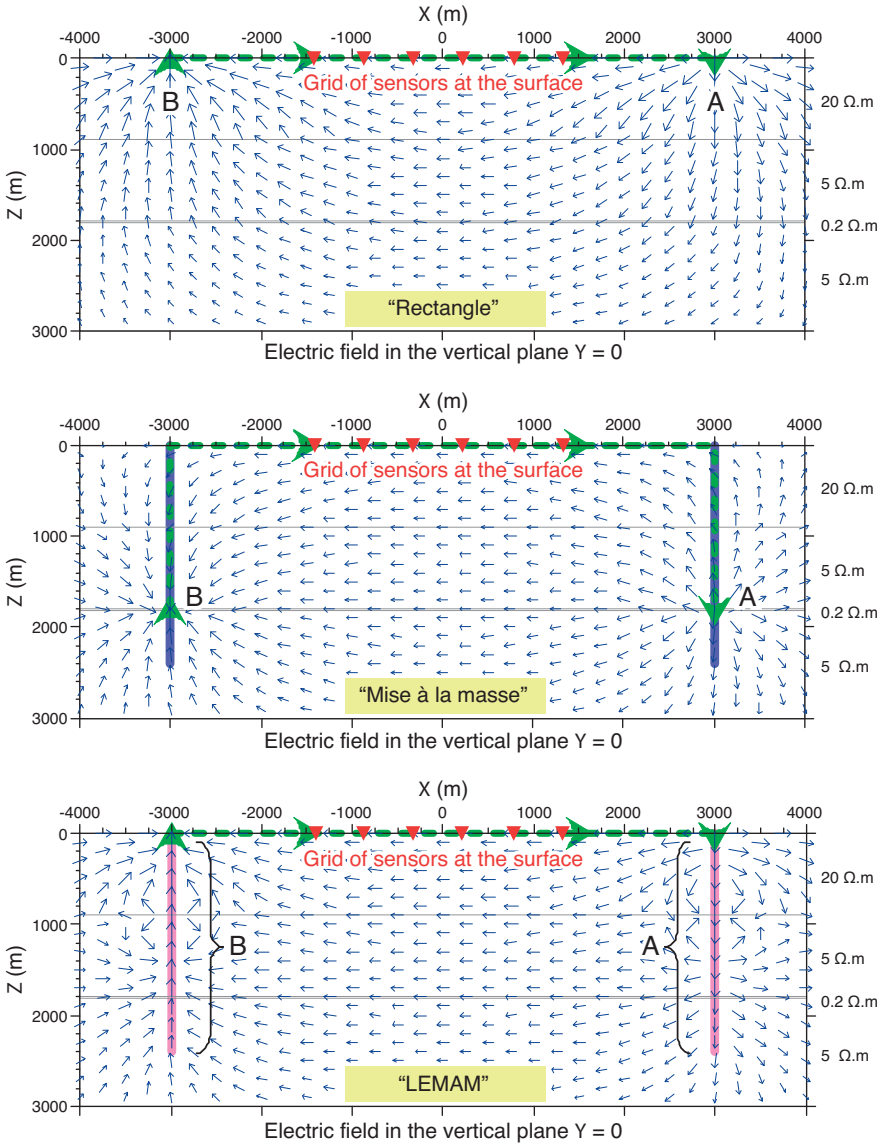

Figure 3

Sketch of three electric injection arrays that can be used for CO_2 monitoring. The blue arrows represent the *E*-field vectors calculated at 0.5 Hz in a 4-layer tabular model without CO_2 plume (*i.e.* the response of the 1D model, or the "layered primary field").

3 NUMERICAL MODELLING

A theoretical study based on 3D numerical modelling has been performed to show the relevance of the LEMAM array for monitoring a CO_2 plume in a deep saline aquifer of the Paris Basin. This work benefited from a parallel study carried out for the In-Salah storage site.

3.1 The Modelling Software

Calculations were performed in the frequency domain with the EM3D software of the University of Utah (Newman and Hohmann, 1988) which uses a volume integral-equation formulation for solving the secondary currents inside bounded heterogeneities of anomalous conductivity. From these currents, the electric and magnetic fields are then computed at any receiver. The interest of this approach is that the discretization is limited to the 3D heterogeneities (the response of the horizontal layers embedding the 3D targets is calculated analytically by Hankel transforms). As a consequence, the number of cells remains moderate, generally in the order of 1000 (to be compared with the 1 000 000 order customary in finite-difference or finite-element modelling, where the whole space must be discretized).

The EM3D code can simulate the response of one or several 3D bodies, each described by a set of adjacent cells having the form of right rectangular prisms parallel to the coordinate axes. For computation purposes, each of these "rectangular cells" is subdivided along each axis into an integer number of "cubic subcells". The size and resistivity of the subcells must be constant over each rectangular cell but can vary from cell to cell (in this study, they are kept constant over each 3D body).

The only physical parameter taken into account in our modelling is the resistivity, both for the cells describing the 3D targets and for the 1D layers. The magnetic susceptibility cannot be accounted for with this software, *i.e.* $\mu = \mu_0$ throughout, and we assume that there is no significant polarisation effect, so the permittivity can be neglected, *i.e.* $\varepsilon = 0$ (in other words, the resistivity is purely real). The source is described by a polygonal wire whose extremities A and B are grounded (*i.e.* galvanic source) and which is traversed by a 1 A time-harmonic current flowing from A to B.

Although some limitations are known for the EM3D software, it is deemed to be quite accurate in calculating a galvanic response such as that expected from a CO_2 bubble.

3.2 The SMB Generic 1D Model

As already said, the area selected for building a resistivity model representative of the south-east of the Paris Basin is located 10 km west of the SMB oilfield (*Fig. 1*), between the villages of Fontenay-de-Bossery (FDB) and Saint-Martin-de-Bossenay (Aube department, Champagne-Ardennes region). The target reservoir for CO_2 storage is the saline aquifer hosted by the Dogger carbonates ("Oolithe Blanche" formation).

3.2.1 The Layered Host

For building our resistivity model, we benefited from the 3D geological model established in 2006 for the south-east of the Paris Basin, within the "PICOREF" RTPG project. An outcome of this work is the geological section shown in Figure 4, which is derived from the borehole information available along the seismic profile EW02 (Robelin, 2008). The strong vertical exaggeration of this figure (about 20:1) illustrates the overall shape of the sedimentary basin. However, if we mentally correct for this exaggeration, we realize that the stratification is essentially horizontal from the surface to the Permian basement, except in the vicinity of the major faults. For example, between SMB and FDB, the deepening of the Bathonian series is only about 200 m for 20 km, *i.e.* a 1% slope. In the selected area, it is thus perfectly legitimate to transform the bent dipping interfaces to straight horizontal interfaces and to work with an equivalent 1D model.

In both Figure 1 and Figure 4, it is worth noting the SMB regional fault, that runs NS in this area and whose throw is about 200 m at the Dogger level. The western compartment of this fault contains the SMB oilfield, trapped by a small anticlinal structure (1 km wide) located close to the fault plane. Our study area is about 10 km west of the SMB oilfield, at a place where the Dogger carbonates are filled with brackish water (saline aquifer). In both figures, the selected area appears to be at fair distance from any major fault, confirming the validity of a 1D model for the EM simulations.

For fixing the resistivity and depth of the model layers, we first reviewed all the geophysical logs available in a 20 km radius around the study area. Among the eight boreholes selected, only four electric logs were found, and these are not complete *(Tab. 2)*. Fortunately, the sections covered by each resistivity log are complementary, which permitted us to build a single composite log covering the entire section from 0 to 3250 m. Self Potential (SP), Gamma-Ray (GR) and sonic (DT) logs were used to correlate the depth sequences between the different boreholes and thus ensure the coherency of the composite log (since at least one of these three ancillary logs is always available for each of the eight boreholes selected). Beyond $Z = 3250$ m, the resistivity of the Permian basement (both detrital and crystalline) was estimated from the lithology, using the scarce descriptions in the literature.

In order to simplify the numerical simulations, the continuous composite log had to be summarized into a sequence of 15 homogeneous layers. In this process, several geological units of nearly identical resistivities were merged to a single layer. Some other zones of rapidly varying resistivity were combined to an equivalent layer having the same longitudinal conductance as the real series.

TABLE 2

Summary of the geophysical logs used for building the resistivity model of the FDB-SMB area. The common depth origin is taken at the head of well SMB 6, the closest to the study area

Borehole name and/or indicator	Electrical Resistivity (LLD or ILD)	Self Potential	Gamma-Ray	Sonic
	Depth range of the log	SP	GR	DT
Val d'Orvin 1 (VOV 1)	1000-1850 m		X	X
Hermé 1D (HRM 1)	1650-3250 m	X	X	X
Fontenay-de-Bossery 1 (FDB 1)			X	X
SMB 6	250-1750 m	X		
SMB 17		X	X	
SMB 18			X	X
Saint-Lupien 1 (SLU 1)	20-600 m	X		
Lepassage 1 (LPS 1)			X	

For a layer of infinite extent in the X, Y directions, the longitudinal conductance (which quantifies the ease of the

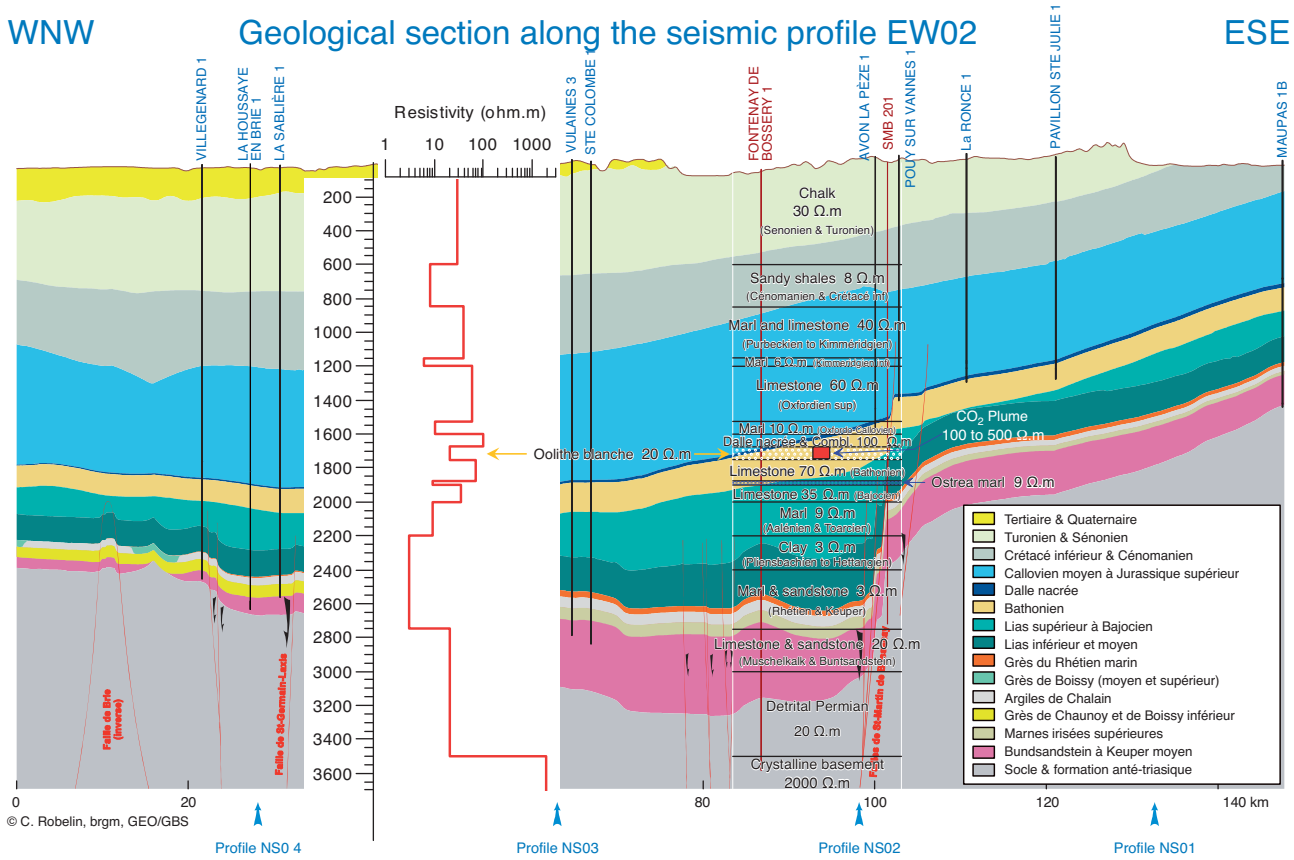

Figure 4

Geological section drawn from the borehole information available along the seismic transect EW02 (adapted from Robelin, 2008). Overlain on top of the section is the generic resistivity model derived from the geophysical logs. In this 15-layer model, the "Oolithe Blanche" formation is the 8th layer, stretching between $Z = 1675$ m and $Z = 1750$ m, with a 20 ohm.m resistivity.

current to flow along the horizontal layer) is defined as the conductivity-thickness product $\sigma\,\Delta z$. The principle of equivalent conductance thus amounts to making a harmonic average of the resistivities in the column, like for resistances connected in parallel:

$$\sigma_{eq}\Delta z = \int \sigma(z)\,dz \quad \Rightarrow \quad \rho_{eq} = \frac{\Delta z}{\int \frac{dz}{\rho(z)}} \tag{7}$$

This approach is perfectly suited to the LEMAM injection, since the injected currents essentially flow along horizontal paths between the long vertical electrodes, like between the plates of a capacitor. It may be remarked that this is not so true for a current injection at the surface (*e.g.* for the RECT array) for which the currents have to follow a substantial vertical path to reach the reservoir depth.

It is noteworthy that the geological units have well-contrasted resistivities in this part of the basin, that is why the simplified resistivity model matches rather well the geology. Some additional rounding of the depths was necessary to ensure that the layer interfaces match the vertical limits of the cells describing the metallic casings (see later), a requirement of the modelling software. When this rounding significantly affected the thickness of a layer, its resistivity was in turn modified so as to keep unchanged the longitudinal conductance. The final 15-layer generic model is shown on top of the geological section in Figure 4, both as a curve (left) and as a 1D section (right). The resistivity and depth values are detailed in Table 3.

3.2.2 The Saline Reservoir

The storage layer considered in this study is the "Oolithe Blanche" formation (Bathonian age), which is both the thickest (≈ 75 m) and the most porous ($\Phi > 0.2$) unit in the Dogger aquifer, and has a permeability suitable for the injection of large volumes of CO_2 ($K \approx 50$ mD)[(2)]. In our model, this

(2) The "Dalle Nacrée" has a higher permeability (≈ 75 mD) but is very thin (17 m) and less porous ($\Phi \approx 0.1$), while the Comblanchien is both less permeable (≈ 25 mD) and less porous ($\Phi \approx 7.5\%$) than the Oolithe Blanche.

TABLE 3

Detailed description of the generic resistivity model for the FDB-SMB area. The storage formation is the 8th layer; the resistivity given in parenthesis corresponds to the case of a more conductive, idealized storage aquifer

Layer number	1	2	3	4	5	6	7	8	9	10	11	12	13	14	15
Depth to top (m)	0	600	850	1150	1200	1525	1600	1675	1750	1875	1900	2000	2200	2750	3500
Depth to bottom (m)	600	850	1150	1200	1525	1600	1675	1750	1875	1900	2000	2200	2750	3500	/
Resistivity (Ω.m)	30	8	40	6	60	10	100	20(1)	70	9	35	9	3	20	2000

formation corresponds to the 8th layer, stretching between $Z = 1675$ m and $Z = 1750$ m. At this depth, the temperature and pressure conditions are largely sufficient to keep the CO_2 in the supercritical state.

Two variants of the reservoir resistivity were compared. The first model, illustrated by Figure 4, was calculated with a realistic reservoir resistivity of 20 ohm.m, reflecting the low salinity of the aquifer in this part of the Basin (≈ 5 g/L of NaCl, *i.e.* brackish water). A second model was calculated with an idealistic reservoir resistivity of 1 ohm.m, corresponding to about 50-70 g/L of NaCl in the aquifer (saline water): though such salinity is not observed anywhere in the Dogger aquifer of the Paris Basin, it is common in other storage aquifers. In the following, the first variant will be called the "realistic SMB model" while the second will be called the "favourable SMB model".

3.3 The 3D CO_2 Plume

After several years at industrial-scale injection rates (> 1 Mt/year), the amount of CO_2 stored in the reservoir will form a large plume (or "bubble") in which the initial pore water has been partly expelled and replaced by supercritical CO_2.

Flow/transport modelling shows that, except in the close vicinity of the injection point, the fluid substitution is only partial: in a homogeneous reservoir, the CO_2 saturation should vary from about 98% at 100 m from the injector ("dried" zone) to approximately 30% at 1 km, for 25 Mt of CO_2 injected in physical conditions typical of the Dogger in this area (André *et al.*, 2007). Using formula (6) with $n = 2$, we can thus anticipate a bubble-to-host resistivity ratio ranging from 2500 in the dried zone to only 2 at 1 km from the injector.

In addition, the actual shape of the plume will be complex, ranging from an upside-down cone in a simple homogeneous medium to intricate digitations in an heterogeneous medium. In this first study, however, the bubble geometry was simplified to a 2 km × 2 km horizontal slab, 70 m thick[3], floating at the top of the oolite *(Fig. 5)*. This body is described by 448 rectangular cells (8 in X, 8 in Y, 7 in Z) of constant shape (250 m × 250 m × 10 m), each subdivided into 625 cubic subcells of 10 m side.

(3) Such a body represents about 25 Mt of CO_2 if a porosity of 20% and a CO_2 saturation of 80% are assumed.

A uniform CO_2 saturation of 80% was assumed within this bubble, resulting in a resistivity contrast of 25 with the initial aquifer (Archie law for $n = 2$). This saturation is certainly exaggerated over such a large scale, and a value of 50-70% would probably be more relevant in average, yielding a resistivity ratio of 5 to 10. However, we know from another ongoing study that the resistivity of the plume is not the most influential parameter governing the response of the plume and so it can be assumed that the responses calculated with this hypothesis have the right order of magnitude.

For the realistic 20 ohm.m reservoir, this hypothesis of saturation leads to a uniform resistivity of 500 ohm.m throughout the bubble, whereas, for the favourable 1 ohm.m reservoir, it means a uniform resistivity of 25 ohm.m.

3.4 The Tx/Rx Configuration

Simulations were performed both for the LEMAM and for the rectangle (RECT) arrays. In the LEMAM models, the current injection was performed by two vertical casings of 2400 m length, separated by a distance of 6 km, located symmetrically about the center of the CO_2 bubble *(Fig. 5)*. Each model was also calculated without these casings, in order to simulate a standard injection at the surface (*i.e.* a RECT array). In order to lessen the influence of the electric wire connecting the injection electrodes, the trajectory of this wire was offset by 2 km in the Y direction.

The electric and magnetic fields were calculated at the ground surface (horizontal plane $Z = 0$) on a 250 × 250 m grid, and on two vertical sections, shown as CD and PQ in Figure 5 (planes $X = 0$ and $Y = 0$), at a 100 m interval along Z.

For the moment, a single frequency, 0.5 Hz, has been simulated. This frequency represents a good compromise between two conflicting issues, the depth of investigation and the spatial resolution. It should be noted that this frequency is right in the frequency range used for marine CSEM (0.1-1 Hz) for targets of similar sizes, depths and electrical characteristics.

3.5 Discretization of the Metallic Casings

The main difficulty in building the LEMAM models is to correctly represent and discretize the well casings used for injecting the electrical current. In the reality, the metallic

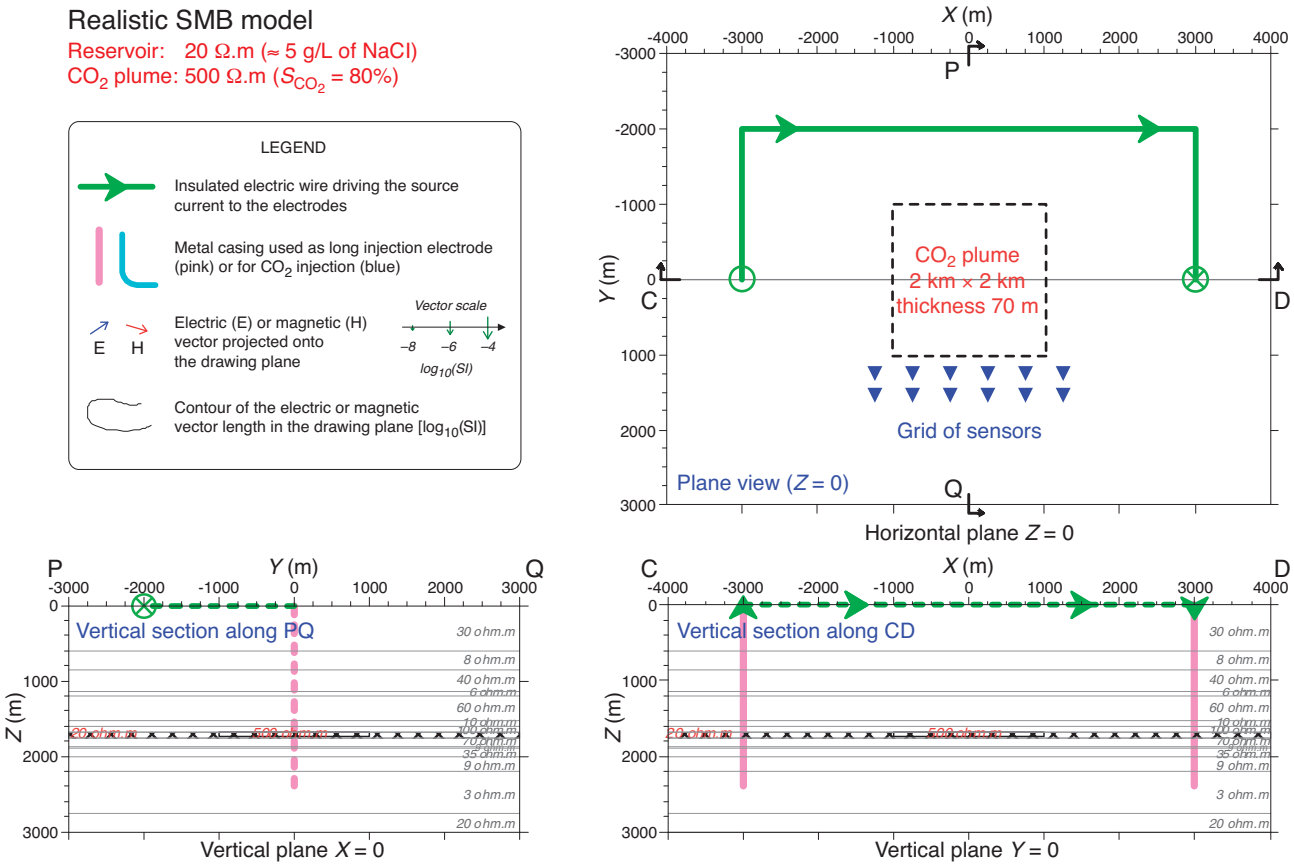

Figure 5

Simplified 3D model used for simulating the LEMAM response of a big CO_2 plume (2 km × 2 km × 70 m) stored in the oolite layer of the Dogger aquifer (realistic version with a 20 ohm.m reservoir and a 500 ohm.m bubble). For simulating the RECT array, the long electrodes must be suppressed. The model is projected on the three natural planes $Z = 0$, $Y = 0$ and $X = 0$.

casings are hollow cylinders that have a resistivity of about 1.7×10^{-7} ohm.m (carbon steel), a wall thickness of about 1 cm, an average diameter of 30 cm (in deep oil wells) and a length of several kilometres. Modelling such geometries at the true scale is not possible: the thin metal section would require the use of very small cells in the horizontal plane, and this in turn would require a gigantic number of cells along the vertical. The only solution is thus to work by equivalence, *i.e.* to replace the real pipes by equivalent long conductors ("pseudo-casings") that can be handled by a standard modelling software like EM3D.

For the SMB model, each casing has been equated to a 2400-m-long vertical prism having a square base of 10 m side. In the horizontal plane, the 10 × 10 m cross-section of the prism is subdivided into four 5 × 5 m rectangular cells (using 5-m-side cubic subcells). Vertically, the casing is subdivided into sections of 50 m height (*i.e.* vertically, a rectangular cell is composed of 10 cubic subcells). A rectangular cell as a whole is thus 5 × 5 × 50 m in X, Y, Z. However, the 50-m vertical discretization has been refined to 25 m within the interval 1500-1900 m to ensure a more detailed description of the currents leaving the casings at the reservoir level. With this discretization, each pseudo-casing is described by 224 rectangular cells.

Once the geometry of the pseudo-casings is defined, it is necessary to determine their equivalent resistivities in such a way that their longitudinal conductance $\sigma \times S$ be the same as that of the real casings (Holladay and West, 1984). Therefore, the equivalent resistivity of the pseudo-casing must verify the equation:

$$S_{eq}/\rho_{eq} = S_{\text{true}}/\rho_{\text{true}}$$

where S_{eq} is the section of the pseudo-casing and S_{true} is the section of the real pipe. Finally, the equivalent resistivity of a 10 × 10 m pseudo-casing is given by:

$$\rho_{eq} = \frac{100 \times 1.7 \times 10^{-7}}{\pi (D - e)\ e} \approx \frac{5.4 \times 10^{-6}}{D\ e}$$

where D is the external diameter of the real pipe, and e its wall thickness. If $D = 0.3$ m and $e = 1$ cm, we get $\rho_{eq} \approx 1.8 \times 10^{-3}$ ohm.m. For convenience, we have rounded this value to

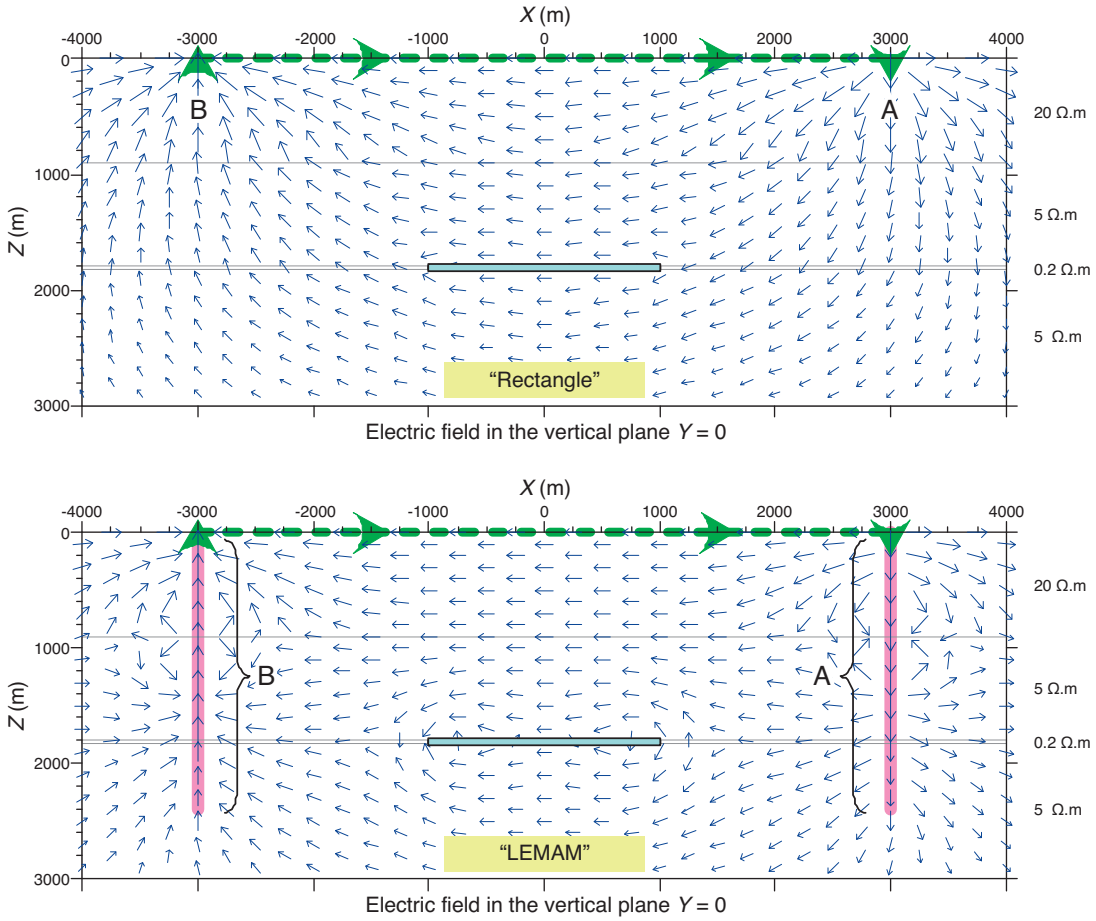

Figure 6

Electric-field distribution around a deep CO_2 bubble for the model of Figure 3, in which a 2 km × 2 km × 20 m bubble of 5 ohm.m (S_{CO_2}= 0.8) has been injected in the 3rd layer, a) for the RECT array and b) for the LEMAM array. The arrows represent the total in-phase vectors at 0.5 Hz.

1.5×10^{-3} ohm.m, but we admit that it could be better to adopt $\rho_{eq} = 2 \times 10^{-3}$ ohm.m or more.

Note that the above equivalence is valid as long as the cross-section of the pseudo-casing remains small compared to the casing length and to the distance between the well and any heterogeneity of interest in the model.

4 MODELLING RESULTS

For each variant of the model (realistic or favourable reservoir), the ***E*** and ***H*** fields were calculated with and without the CO_2 plume, and the difference between these two states represents the time-lapse response of the plume. At each receiving point at the ground surface (or in a vertical section), this response is then normalized by the magnitude of the field existing at the same point without the CO_2 plume (*i.e.* initial field before injection).

For presenting the modelling results, we will adopt the following terminology, valid for both the ***E*** and ***H*** fields:

- the field calculated without CO_2 plume, for a given array (RECT or LEMAM), is called the primary field (***Ep***) for this array; in field operations, it corresponds to the initial field, or "baseline" measured before CO_2 injection;
- the field calculated in the presence of the plume for the same array is called the total field (***Et***); it corresponds to the final field measured after CO_2 injection, during a second iteration of the field survey;
- the difference between the total field and the primary field is called the secondary or reduced field (***Er***); it corresponds to the time-lapse response of the CO_2 plume for the considered 1D model and Tx array (***Er*** = ***Et*** – ***Ep***).

In field operations, the reduced field will be obtained as the difference between the final field and the initial field. Equating this difference to the time-lapse response of the CO_2 plume needs to assume that the only resistivity variation

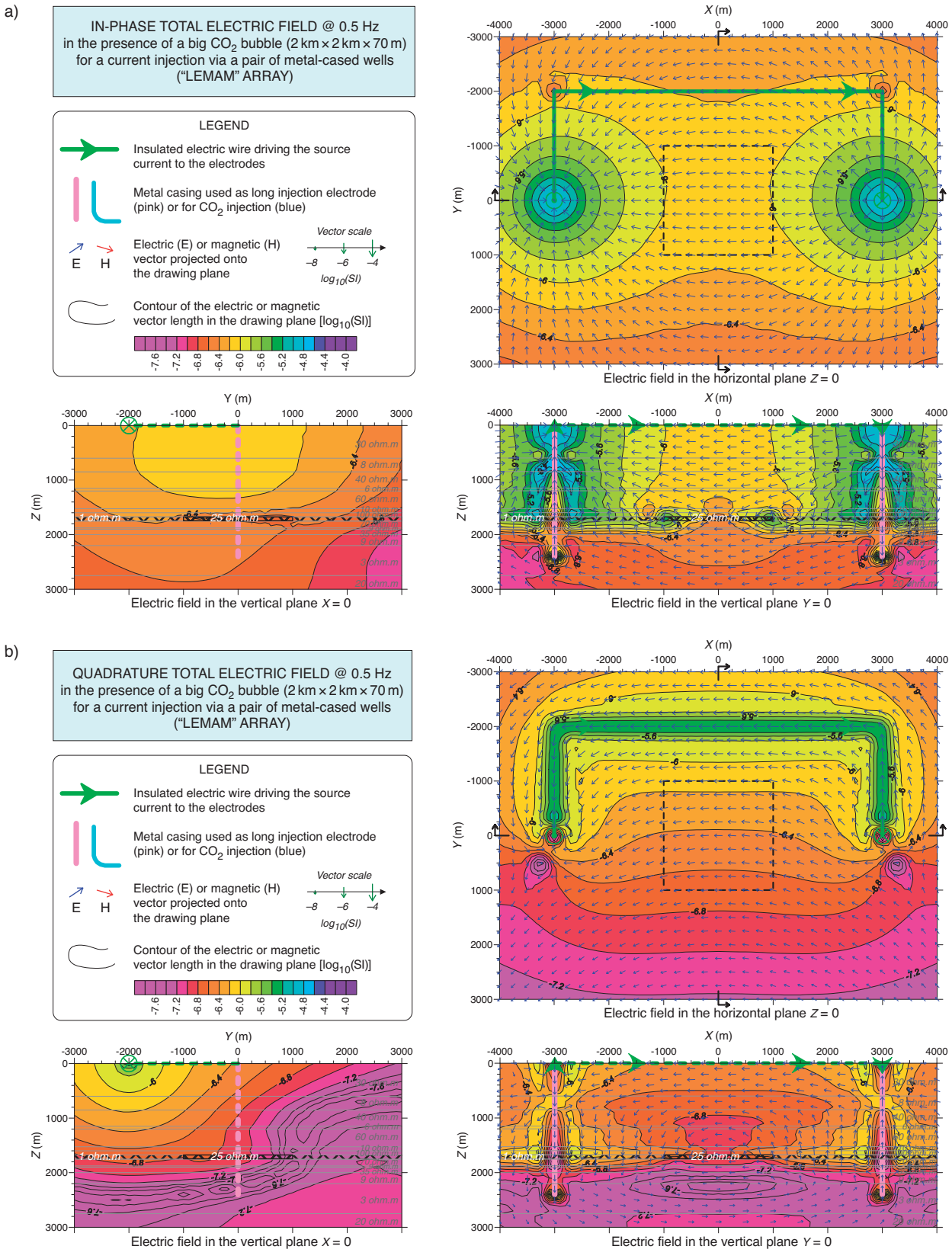

Figure 7

Total electric field calculated for a LEMAM injection at 0.5 Hz with the model defined in Figure 5, in which the reservoir is at 1 ohm.m instead of 20 and the CO_2 bubble at 25 ohm.m instead of 500 ("favourable model"). a) In-phase field, b) quadrature field.

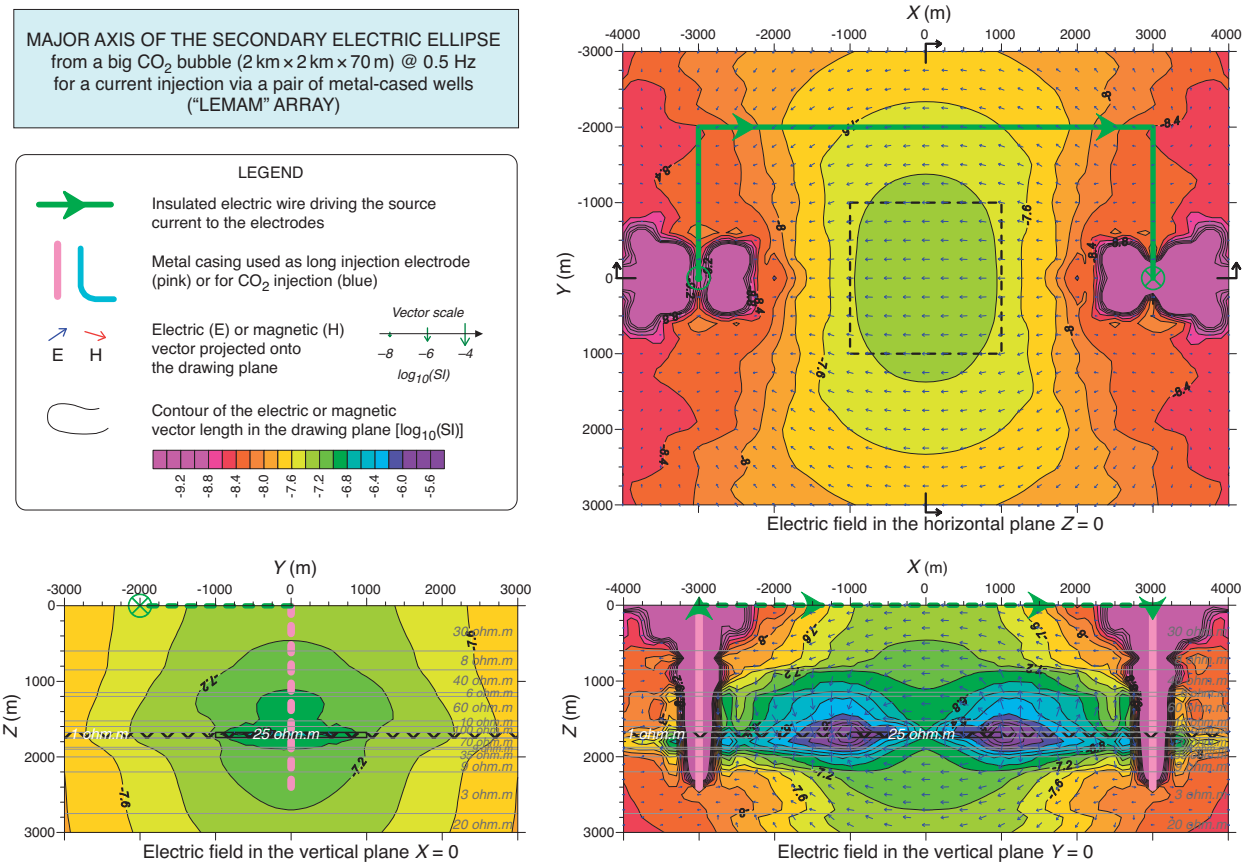

Figure 8

Major axis of the secondary electric field from the CO_2 bubble defined in Figure 5, for a favourable reservoir of 1 ohm.m and a 25 ohm.m bubble, for a LEMAM injection at 0.5 Hz.

occurring between the two survey repetitions is due to the fluid substitution within the plume (any other resistivity variation is supposed to have a negligible effect at the measuring stations at the ground surface).

Like any harmonic signal, each of the three geometric components of the electric (or magnetic) field is associated with a complex number (phasor) that can be decomposed into a real (or in-phase) part and an imaginary (or quadrature) part. The common phase reference of all the signals is supposed to be given by the source current. For field measurements, this implies that the transmitter and the receiver be adequately synchronized, for example by GPS signals.

The combination of three orthogonal complex components having individual phases defines an elliptic polarization, *i.e.* the 3-component vector describes a planar ellipse built on the in-phase and quadrature real vectors. The semi-major axis of this ellipse is a new real vector that summarizes the other two vectors *(Fig. 8)* and that can be used instead of them to describe the complex field in a more relevant manner, since its magnitude gives a true measure of the field strength, and since it is an invariant, independent on the phase origin. In the following, we will omit the prefix "semi-" and simply designate this vector as the "major axis".

The primary field is not shown in the following figures, since it represents solely the response of the 1D model to the injected current. However, this initial field is used for normalizing the time-lapse response of the CO_2 bubble. For example, if we are dealing with the major axis of the time-lapse electric response ($\boldsymbol{Er}_{ma}$), we will normalize this field by the length of the major axis of the initial electric field, $\boldsymbol{Ep}_{ma}$ and will plot the relative time-lapse response defined as: $Er_{ma}(\%) = 100 \times \|\boldsymbol{Er}_{ma}\|/\|\boldsymbol{Ep}_{ma}\|$ *(Fig. 9)*.

This normalization is very important in order to establish whether or not the detection and mapping of the target will be possible. In practice, the reduced field needs to be above a certain percentage of the initial field in order to be detectable over the repetition noise. This constraint is common to all controlled-source frequency-domain methods, in which the target response is measured concurrently with the primary

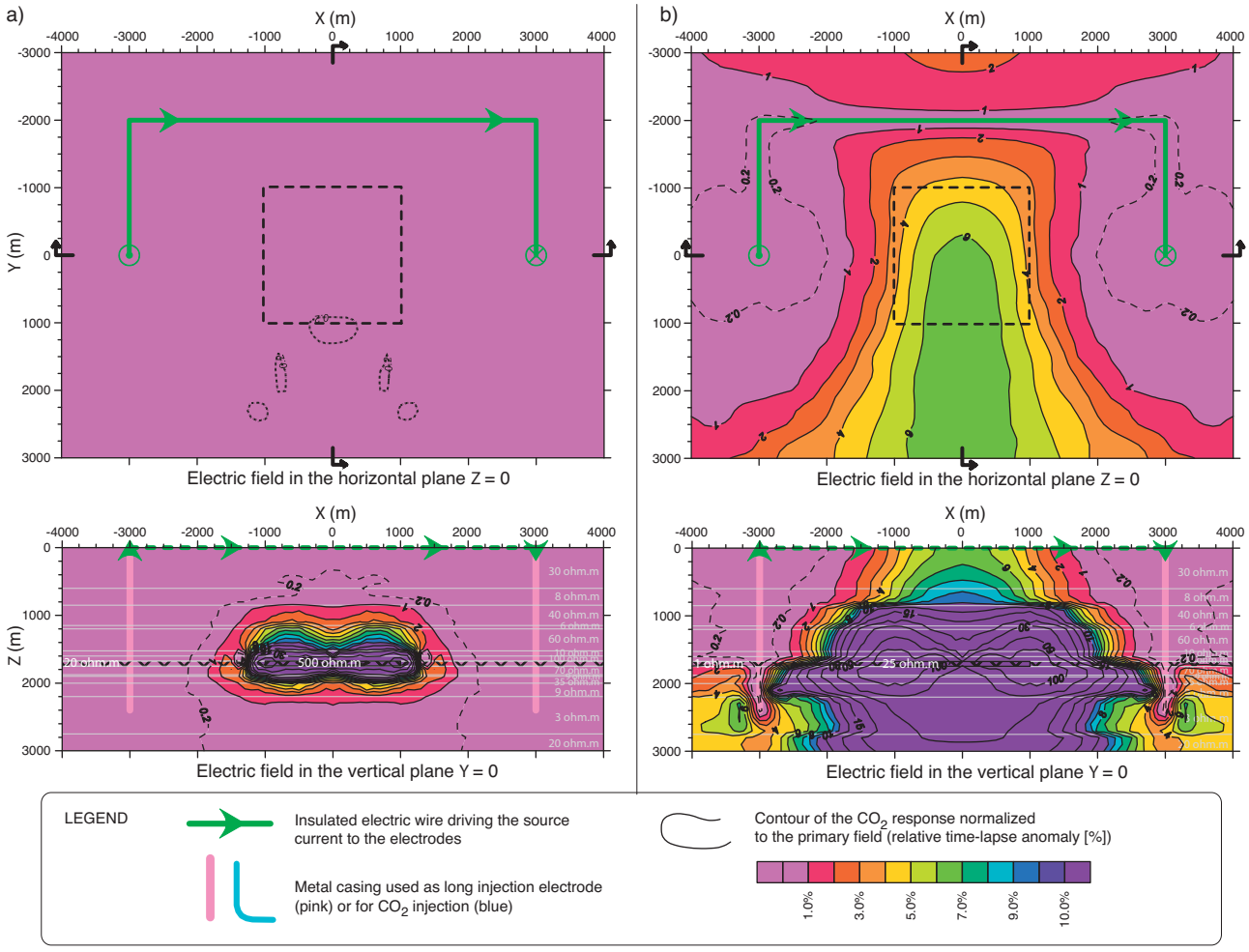

Figure 9

Relative time-lapse electric response (major axis) from the CO_2 bubble defined in Figure 5 for a LEMAM injection at 0.5 Hz for two variants of the reservoir layer: a) for a realistic reservoir of 20 ohm.m; b) for a favourable reservoir of 1 ohm.m.

field. The overall repetition noise will depend on repositioning errors and on external causes such as near-surface resistivity variations. A common noise threshold adopted in electrical exploration methods is 1% of the primary field (Levesque, 2006, *Fig. 3*). This threshold can be reduced if a special care is taken in controlling the geometry of the system (certain airborne EM systems announce an effective noise threshold of 10 ppm). The question is presently under investigation, so for the moment we will assume a noise threshold of 1%.

As already said, in order to compare the respective performances of the RECT and LEMAM arrays, each model was calculated for the two types of current injection. Figure 6 compares the electric field vectors for the two configurations and clearly shows that the LEMAM array reacts much more strongly to the CO_2 bubble than does the RECT array: with the LEMAM array, the vectors are strongly distorted around the CO_2 bubble, whereas with the RECT array the distortion is hardly visible.

The total electric field obtained with the favourable SMB model (*i.e.* 1 ohm.m reservoir with a 25 ohm.m bubble), for a LEMAM injection at 0.5 Hz, is displayed in Figure 7. Even if the CO_2 bubble gives a strong response in this case (see later), there is absolutely no evidence of the bubble on the total field at the ground surface: in the plane $Z = 0$, the in-phase field is similar to that of a DC injection in a homogeneous half-space, and the quadrature field is mainly influenced by inductive effects in the vicinity of the insulated cable that connects the long electrodes.

For this same model (again with the favourable reservoir), Figure 8 illustrates the time-lapse electric response of the CO_2 bubble, in the form of a plot of the major axis of the

reduced electric field. The surface anomaly due to the CO_2 injection shows a well-defined maximum centred on the target. The magnitude contour (yellow-to-green) that matches the bubble limits is about $10^{-7.4}$ V/m, whereas the natural Magneto-Telluric (MT) noise at 0.5 Hz should be less than 10^{-8} V/m in the worst case. This represents a *S/N* ratio of more than 4, which is already sufficient to get good data. However, we must remember that the results plotted in Figure 8 are calculated for a 1 A injection, while the field data should normally be recorded with more than 10 A in the source: the electric response being proportional to the injected current, the *S/N* ratio should thus be about 40, which is very comfortable indeed.

Figure 9b displays the previous time-lapse electric response (major axis) after normalization by the major-axis length of the primary field. Despite the distortion due to the inductive effects close to the connecting wire, it appears that the relative time-lapse anomaly at the surface, in the case of the favourable reservoir, is between 4 and 6% of the initial field above the bubble, which is quite measurable. This good result is explained by the fact that the reservoir, in this case, is the most conductive layer of the model *(Tab. 3)* and thus it channels an important part of the injected current (about 30%) that in turn energizes the plume.

Similarly, Figure 9a displays the relative time-lapse electric response in the case of the realistic SMB model (20 ohm.m reservoir with a 500 ohm.m bubble, as illustrated in *Fig. 5*). In this case, the relative time-lapse response at the surface appears to be less than 0.5% of the initial electric field, which is below the estimated "repetition noise". This poor result can be understood by the fact that the reservoir, in this case, is far from being the most conductive layer of the model *(Tab. 3)*. As a consequence, only a minor part of the injected current is used for energizing the plume: it is estimated that only about 2% of the injected current crosses the reservoir, hence the poor response of the plume.

Though the 1% threshold that we have adopted is still provisional and has to be better estimated during the first field tests, it seems that the low salinity of the aquifer in this area is not appropriate for the LEMAM method, at least at this frequency.

It is worth noting that the time-lapse response also depends on the length of the well casings below the reservoir and on the conductivity of the layers intersected underneath. In our model, the casings exceed the reservoir bottom by 650 m (a situation that can occur in practice), while very conductive layers are intersected in this depth interval (*e.g.* layer No. 10 and 12, with $\rho = 9$ ohm.m; layer No. 13, with $\rho = 3$ ohm.m, *Tab. 3*). This situation is not ideal since a significant part of the source current is injected in these superfluous casing portions, leaving less useful current for the reservoir. Using a rough calculation, we have estimated (again for the realistic model) that the current injected in the reservoir would increase to about 5% of the source current if the well casings were stopped at the reservoir bottom[4] (to be compared with the previous 2%). Similarly, for the favourable model, the current ratio would increase to 50%, instead of the previous 30%.

For illustrating the superiority of the LEMAM array over the RECT array, Figure 10a shows the relative electric response obtained with the RECT array for the same favourable model. It appears that the relative time-lapse anomaly at the surface is about 1-2% of the initial field, confirming the intuition that the CO_2 response should be hardly measurable using a surface-to-surface array.

Coming back to the LEMAM injection, Figure 10b illustrates the relative magnetic anomaly corresponding to the favourable model. This figure shows that the magnetic response obtained for the LEMAM injection is about 2-3% of the initial magnetic field. It is thus smaller than the electric response and it seems also more influenced by inductive effects around the connecting wire. This tends to indicate that the magnetic field has less interest than the electric field for monitoring a CO_2 injection, which is consistent with the theory of a galvanic response.

CONCLUSION

This modelling study on the applicability of EM methods to the monitoring of a deep CO_2 injection gives promising results. For a CO_2 storage at 1700 m depth in the Dogger aquifer, the use of long metallic casings for injecting the source current into the ground (in the so-called LEMAM array) permits to multiply by a factor of three the time-lapse electric response of the CO_2 plume at the surface (by comparison to a standard short-electrode injection). A similar or even greater increase is observed for the magnetic response (not developed here). As a result, in the LEMAM configuration, the time-lapse response of the modelled plume is well above the estimated repetition noise ($\approx 1\%$) and is thus measurable (yet under certain assumptions), which is not the case with short electrodes.

However, the study also shows that the LEMAM method will not be applicable in every situation. For the method to be successful, the storage formation must be one of the most conductive layers intersected by the long electrodes, so that a significant fraction of the current be injected at the reservoir depth and energizes the plume. This is illustrated by the two versions of our resistivity model:

– for the realistic SMB aquifer (water salinity ≈ 5 g/L, reservoir resistivity 20 ohm.m), the current injected in the reservoir is only about 2% of the total injected current; in this case, the CO_2 response is less than 0.5% of the initial field, which is not measurable;

(4) This does not mean, however, that the relative time-lapse response will be detectable over the repetition noise.

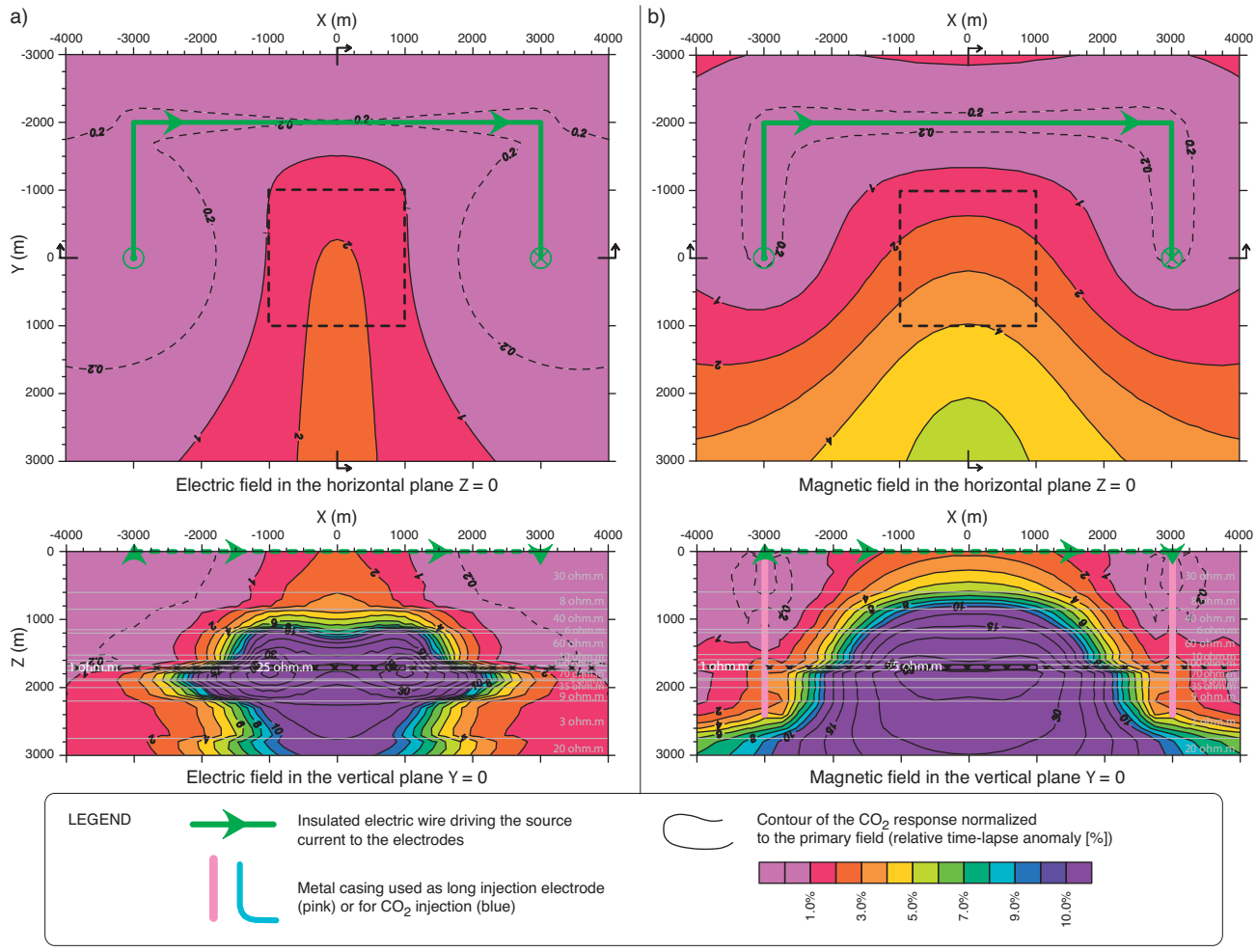

Figure 10

Relative time-lapse response (major axis) obtained at 0.5 Hz from the CO_2 bubble defined in Figure 5, again for a favourable reservoir of 1 ohm.m and for a 25 ohm.m bubble: a) for the electric field with a RECT array; b) for the magnetic field with a LEMAM array.

– in contrast, for the idealized SMB aquifer (water salinity 50-70 g/L, reservoir resistivity 1 ohm.m), the current injected in the reservoir is about 30% of the total injected current; as a result, the CO_2 response is more than 6% of the initial field, and is thus quite measurable.

From these observations, it is estimated that the current injected in the reservoir should be at least 10% of the total injected current in order to get a measurable CO_2 response at the surface. This threshold will be refined through further modelling.

The above results open the way for new researches on the application of EM methods to CO_2 monitoring. In particular, it would be useful to establish simple rules permitting to quickly determine the applicability of the LEMAM method to a given storage site, according to its electrical characteristics (resistivity and thickness of the geological layers, geometry of the injection array). We can already anticipate that the most influential parameters are the conductivity and thickness of the reservoir layer (*i.e.* its conductance), compared to the overall conductance of the layers intersected by the long electrodes.

ACKNOWLEDGMENTS

This work was supported by the French National Research Agency (ANR) under programme "*Captage et Stockage du* CO_2", as part of the project "Géocarbone-Monitoring" (ANR 05-CO_2-008, 2006 to 2008). It benefited from a parallel study carried out for the In-Salah site within the CO_2ReMoVe project (2006-2011) under the European FP6 programme. Special thanks are given to Sandrine Grataloup

and Christian Robelin (BRGM Geological Service) for making available to us the geological/structural syntheses performed on this part of the Paris Basin within the PICOREF projects (RTPG 2005-2006; ANR-CO_2 2006-2008). This work continues in a new project started in 2008, "EMSAP-CO_2" that is also supported by the CO_2 programme of the French ANR.

REFERENCES

André L., Audigane P., Azaroual M., Menjoz A. (2007) Numerical modelling of fluid-rock chemical interactions at the supercritical CO_2-liquid interface during CO_2 injection into a carbonate reservoir, the Dogger aquifer (Paris Basin, France), *Energ. Convers. Manage.* **48**, 6, 1782-1797.

Archie G.E. (1942) The electrical resistivity log as an aid in determining some reservoir characteristics, *Am. Inst. Min. Metallurg. Petr. Eng., Tech. paper* 1422, **146**, 54-62.

Bourgeois B., Suignard K., Perruson G. (2000) Electric and magnetic dipoles for geometric interpretation of three-component electromagnetic data in geophysics, *Inverse Probl.* **16**, 1225-1261.

Daily W., Ramirez A., Newark R., Masica K. (2004) Low-cost reservoir tomographs of electrical resistivity, *Leading Edge* **23**, 472-480.

Hatanaka H., Tetsuo A., Mizunaga H., Ushijima K. (2005) Three-dimensional modelling and inversion of the Mise-à-la-Masse data using a steel-casing borehole, *Proceedings of the World Geothermal Congress*, Antalya, 24-29 April 2005.

Holladay S., West G.F. (1984) Effect of well casings on surface electrical surveys, *Geophysics* **49**, 177-188.

Kauahikaua J., Mattice M., Jackson D. (1980) Mise-à-la-Masse mapping of the HGP-A geothermal reservoir, Hawaii, *Geothermal Resour. Council T.* **4**, 65-68.

Levesque C. (2006) Crosswell electromagnetic resistivity imaging: illuminating the reservoir, *Middle-East Asia Reservoir Rev.* **7**, 24-33 (*Schlumberger* brochure on crosswell EM).

Newman G.A., Hohmann G.W. (1988) Transient electromagnetic responses of high contrast prisms in a layered earth, *Geophysics* **53**, 691-706.

Newmark R.L., Ramirez A.L., Daily W.D. (2001) Monitoring carbon dioxide sequestration using Electrical Resistance Tomography (ERT): sensitivity studies, *First National Conference on CO_2 sequestration*, Washington, DC, May 2001.

Robelin C. (2008) Projet PICOREF - Géométrie des principales surfaces géologiques dans le sud-est du Bassin de Paris, *BRGM report* (in press).

Rocroi J.P., Koulikov A.V. (1985) The use of vertical line sources in electrical prospecting for hydrocarbon, *Geophysical Prospect.* **33**, 138-152.

Sill W.R., Ward S.H. (1978) *Electrical energizing of well casings*, University of Utah, Department of Geology and Geophysics, Final Report, Vol. 77-8, 10 p.

Supriyanto S., Daud Y., Sudarman S., Ushijima K. (2005) Use of Mise-à-la-Masse survey to determine new production targets in Sibayak field, Indonesia, *Proceedings of the World Geothermal Congress*, Antalya, 24-29 April 2005.

Waxman M.H., Smits L.J.M. (1968) Electrical conductivities in oil-bearing shaly sands, *Soc. Petrol. Eng. J.* **8**, 107-122.

Final manuscript received in April 2009
Published online in July 2010